This article has been accepted for publication in a future issue of this journal, but has not been fully edited. Content may change prior to final publication. Citation information: DOI 10.1109/TNSRE.2016.2627809, IEEE Transactions on Neural Systems and Rehabilitation Engineering

Imagined Hand Clenching Force and Speed Modulate Brain Activity and are Classified by NIRS Combined with EEG

Yunfa Fu, Xin Xiong, Changhao Jiang, Baolei Xu, Yongcheng Li, and Hongyi Li

***Abstract*—Simultaneous acquisition of brain activity signals from the sensorimotor area using NIRS combined with EEG, imagined hand clenching force and speed modulation of brain activity, as well as 6-class classification of these imagined motor parameters by NIRS-EEG were explored. Near infrared probes were aligned with C3 and C4, and EEG electrodes were placed midway between the NIRS probes. NIRS and EEG signals were acquired from 6 healthy subjects during 6 imagined hand clenching force and speed tasks involving the right hand. The results showed that NIRS combined with EEG is effective for simultaneously measuring brain activity of the sensorimotor area. The study also showed that in the duration of (0, 10) s for imagined force and speed of hand clenching, HbO first exhibited a negative variation trend, which was followed by a negative peak. After the negative peak, it exhibited a positive variation trend with a positive peak about 6–8 s after termination of imagined movement. During (-2, 1) s, the EEG may have indicated neural processing during the preparation, execution, and monitoring of a given imagined force and speed of hand clenching. The instantaneous phase, frequency, and amplitude feature of the EEG were calculated by Hilbert transform; HbO and the difference between HbO and Hb concentrations were extracted. The features of NIRS and EEG were combined to classify 3 levels of imagined force (at 20/50/80 % MVGF (maximum voluntary grip force)) and speed (at 0.5/1/2 Hz) of hand clenching by SVM. The average classification accuracy of the NIRS-EEG fusion feature was 0.74 ± 0.02. These results may provide increased control commands of force and speed for a brain-controlled robot based on NIRS-EEG.**

***Index Terms*—Brain-computer interface, electroencephalogram (EEG), near infrared spectroscopy (NIRS), imagined force and speed of hand clenching, NIRS-EEG.**

This work was supported by the National Natural Science Foundation of China under Grant 81470084, 61463024 and 61363043, by the Applied Basic Research Foundation of Yunnan Province under Grant 2013FB026, by the Cultivation Program of Talents of Yunnan Province under Grant KKSY201303048, by the Focal Program for Education Office of Yunnan Province under Grant 2013Z130. *(Corresponding author: Yunfa Fu).*

Yunfa Fu was with the State Key Laboratory of Robotics, Shenyang Institute of Automation (SIA), Chinese Academy of Sciences (CAS). He is currently with the Automation Department, Faculty of Information Engineering and Automation, Kunming University Science and Technology and the Institute of Brain Information Processing and Brain-computer Interaction Fusion Control, Kunming University Science and Technology, Kunming, 650500 China (e-mail:fyf@ynu.edu.cn).

Xin Xiong is with the Biomedical Engineering Department, Faculty of Information Engineering and Automation, Kunming University Science and Technology and the Institute of Brain Information Processing and Brain-computer Interaction Fusion Control, Kunming University Science and Technology, Kunming, 650500 China.

Changhao Jiang is with the Beijing Municipal Key Laboratory of Evaluation and Technical Analysis of Motor Function and the Brain Science and Sports Laboratory of Capital Institute of Physical Education, Beijing, 100088 China.

Baolei Xu was with the State Key Laboratory of Robotics, Shenyang Institute of Automation (SIA), Chinese Academy of Sciences (CAS). He is currently with Nanjing HUAWEI Research Institute, Nanjing, 210000 China.

Yongcheng Li is with the State Key Laboratory of Robotics, Shenyang Institute of Automation (SIA), Chinese Academy of Sciences (CAS), Shenyang, 110016 China.

Hongyi Li is with the State Key Laboratory of Robotics, Shenyang Institute of Automation (SIA), Chinese Academy of Sciences (CAS), Shenyang, 110016 China.

I. Introduction

Although EEG has low spatial resolution, it continues to be a valuable tool for research and diagnosis, especially when millisecond-range temporal resolution, such as brain-computer interaction applications (not possible with MRI) is required. Compared with EEG, NIRS is an active measuring method to emit energy into tissue and infer functional neural activity from metabolic activity, which is measured by changing light absorption [1]-[3] and is a relatively new approach in neuroscience and brain-computer interfaces [4]-[8]. With fNIRS, tissue function alone produces the imaged signal [9]. Though NIRS has a low time resolution, it has a stronger anti-interference ability (e.g., electrical noise) and a relatively stable signal compared to EEG [2], [3], [6], [10]. The above 2 methods to detect noninvasively brain activity on the scalp have pros and cons. Whether combining these 2 detection methods compensates for their limitations remains to be investigated. For this purpose, this study proposes a method in which brain signals from the same cortical areas (sensorimotor area) can be acquired simultaneously by NIRS combined with EEG. This method may provide support for multi-mode brain computer interfaces based on NIRS-EEG [10]-[13].

In addition, studies have shown that both actual movement and motor imagery can modulate EEG [14]-[19] and NIRS activity [20]-[26]. However, it remains to be determined whether imagined hand clenching force and speed can modulate NIRS and EEG signals. For this reason, this study investigated imagined hand clenching force and speed modulation of NIRS and EEG under the proposed motor parameters imagery (MPI) paradigm based on the above NIRS-EEG acquisition method [10].

Finally, decoding of imagined movement parameters based on central nerve signals collected by non-invasive methods may provide increased and flexible control command numbers for BCI applications [10], [27], [28]. However, this is a great challenge. It is difficult to obtain stable and good classification accuracy using the traditional single mode or single feature

This article has been accepted for publication in a future issue of this journal, but has not been fully edited. Content may change prior to final publication. Citation information: DOI 10.1109/TNSRE.2016.2627809, IEEE Transactions on Neural Systems and Rehabilitation Engineering

method (such as EEG or NIRS). It is well known that the advantage of using EEG and NIRS in a hybrid BCI system is either to improve classification accuracy or to increase the number of control commands. Some progress in decoding motor attempt and imagery or movement directions using NIRS-EEG has been made [10], [29-31]. Yin et al. separated hand clenching force from speed motor imagery and achieved clear results [10]. However, different levels of hand clenching force and speed motor imageries were not decoded. In this study, we attempted to classify 3 levels of imagined hand clenching force and speed motor parameters (a total of 6 classes) by NIRS combined with EEG.

II. Materials and methods

A. Subjects

Six healthy volunteers (S1–S6; 3 men and 3 women; age 24–33 years and mean age 26.8 ± 3.3 years; all right-handed) participated in NIRS and EEG data acquisition. Three subjects had not been in an NIRS experiment previously, and 4 subjects had not been in an EEG experiment previously. None had known sensory-motor diseases or history of psychological disorders. Each subject gave informed consent for the study, which was approved by Shenyang Institute of Automation (SIA), Chinese Academy of Sciences.

B. Experimental paradigm: mental task and timing for a trial

The subjects were asked to execute 6 imagery tasks: imagined speed of hand clenching self-paced movements involving the right hand at 0.5 Hz (slow), 1 Hz (normal), and 2 Hz (fast) rate as well as imagined force of hand clenching self-paced movements involving the right hand at 20% (low), 50% (middle), and 80% (high) maximum voluntary hand clenching force (MVGF). Fig. 1 shows the timing diagram of a single trial for imagined force and speed of hand clenching during brain signals simultaneously acquired by NIRS combined with EEG. The top panel in Fig. 1 shows 3 modes of variation in force of hand clenching, including the development rate of 20%, 50%, and 80% MVGF during 2 s for target force of hand clenching (TGF) and then keeping TGF constant for 8 s; the middle panel in Fig. 1 shows cue presentation for imagined force and speed of hand clenching; the bottom panel in Fig. 1 shows timing of a single trial for mental tasks. The timing diagram was generated by E-Prime 1.1 (Psychology Software Tools, Inc., Sharpsburg, KY, USA).

C. Imagined hand clenching force and speed training for subjects

Before formal data acquisition, all subjects were instructed to understand the instructions of imagined hand clenching at a specific speed or force. Subsequently, they were first asked to execute 3 modes of actual hand clenching movement at a speed of 0.5/1/2 Hz with the metronome program pacing in order to experience each speed movement and then imagine hand clenching speed movement with and without the cue from the metronome program (self-paced). Subjects who were instructed to focus on the right hand during motor imagery executed kinesthetic imagination from the first person perspective (to recall and feel his/her own right hand and mainly experience the mental rehearsal of an actual hand clenching movement

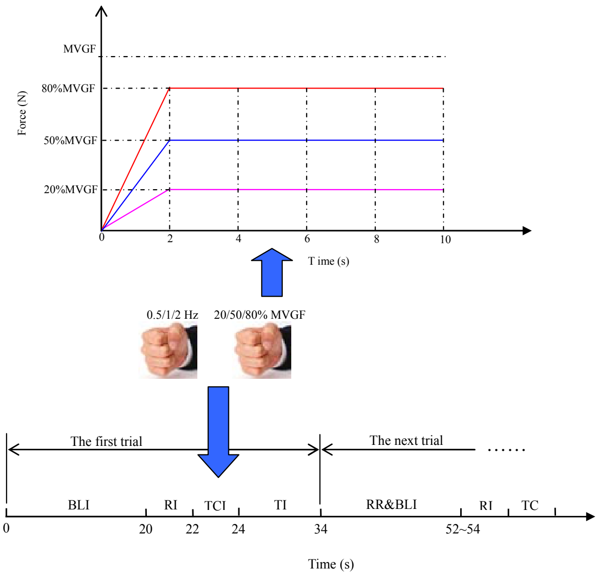

Fig. 1. Timing schematic diagram of a single trial for imagined force and speed of hand clenching during brain signals simultaneously acquired by NIRS combined with EEG. In the timing diagram: baseline interval (BLI), ready interval (RI), task cue interval (TCI/TC), task interval (TI), and random rest (RR). Here, the time instant 0 was the starting moment of the experiment.

without overt movement), avoiding any visual imagery from the third person perspective (i.e., see a motion picture in mind). The subjects were asked to relax, avoid body muscle activity, facial muscle tension, blinking, and slow eye movement during motor imagery.

For imagined force of hand clenching, MVGF was first determined as the average of 3 maximal force of isometric hand-clenching with the hand dynamometer, which were separated by 3 min rest intervals. After calculating MVGF, the subjects were asked to execute the actual hand clenching force movement with the hand dynamometer according to 3 target hand clenching force (20/50/80% MVGF) requirements: development for 2 s, keeping constant for 8 s, and executing the corresponding force of hand clenching motor imagination using kinesthetic imagery. For the above 6 types of force and speed of hand clenching motor imagery, the subjects were trained until they reported imagined movements with a clear, vivid, and controllable effect [32].

D. Positioning of NIRS probes and EEG electrodes for NIRS combined with EEG

To measure simultaneously variations in EEG related to mental tasks and corresponding variations in NIRS, near infrared probes were aligned with C3 or C4, and reference and EEG electrodes were located midway between the NIRS probes as shown in Fig. 2. The EEG recording was referenced to the bilateral mastoid (M1, M2) and grounded at Fpz. Electrodes were made of Ag-AgCl powder.

E. The synchronous method and experimental setup for simultaneous acquisition of NIRS-EEG

While the cued picture for motor imagery task was presented to a subject, the cued signal was simultaneously sent to the EEG

This article has been accepted for publication in a future issue of this journal, but has not been fully edited. Content may change prior to final publication. Citation information: DOI 10.1109/TNSRE.2016.2627809, IEEE Transactions on Neural Systems and Rehabilitation Engineering

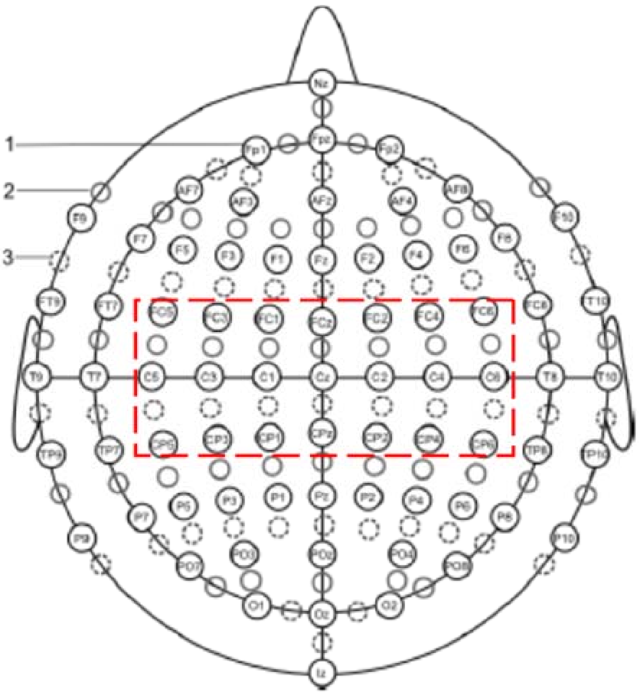

(a)

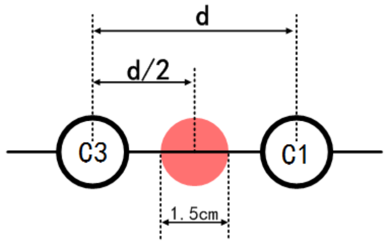

(b)

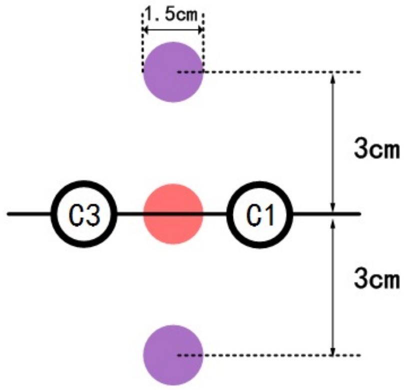

(c)

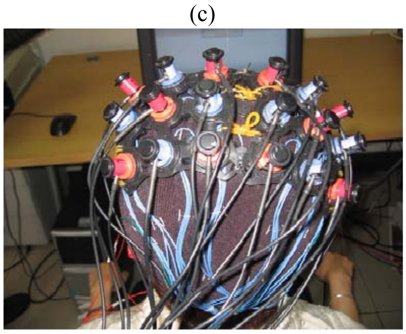

(d)

Fig. 2. Positioning of NIRS probes and EEG electrodes for NIRS combined with EEG. (a) The electrode-optode arrangement surrounded by a red dashed line for the recording region of the experiment. Labels 1, 2, and 3 indicate the EEG electrode, near infrared emitting probe, and receiving probe, respectively. (b) Schematic diagram of the round red hole position. (c) Schematic diagram of the round blue hole position. The round red and blue hole positions for near infrared probes were aligned with C3 for the simultaneous measurement of EEG and NIRS. The round red and blue hole positions represent the drilling hole positions on the EEG cap for near infrared probes. (d) The actual positions of the EEG electrodes and the NIRS probes in the experiment.

and NIRS amplifier to achieve synchronous acquisition. The cue signal for the EEG acquisition system (Neuroscan SynAmps2, Charlotte, NC, USA) was sent by the parallel port, and after 50 ms, the signal 0 was sent to reset. The trigger signals were 1, 2, 3, 4, 5, and 6 (corresponding to the 6 motor imagery tasks). The cue signal for the ETG-4000 (Hitachi Medical Corporation, Tokyo Japan) was sent by the serial port and its source was set on ETG-4000.The trigger signals were F1, F2, F3, F4, F5, and F6 (also corresponding to the 6 motor imagery tasks). In the experimental process, to reduce the time difference between the above 2 cue signals, the trigger was first sent to the ETG-4000 by the serial port and then to the SynAmps by the parallel port. The time difference between the 2 triggers measured by the experiment was 1–2 ms, which was in the acceptable range. Synchronous acquisition of EEG and cerebral blood oxygen signal is shown in Fig. 3(a).

The data were recorded only when EEG and NIRS amplifiers were activated and the subjects performed self-paced hand clenching force and speed motor imagery according to a cue provided by the timing of experiments. Extraction and analysis of the data segments were based on the synchronized signal and the timing of experiments.

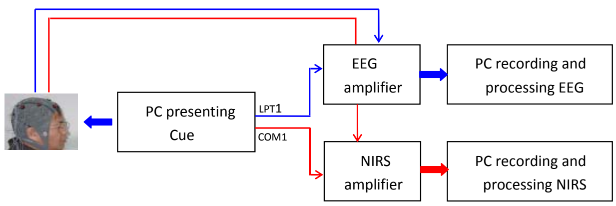

(a)

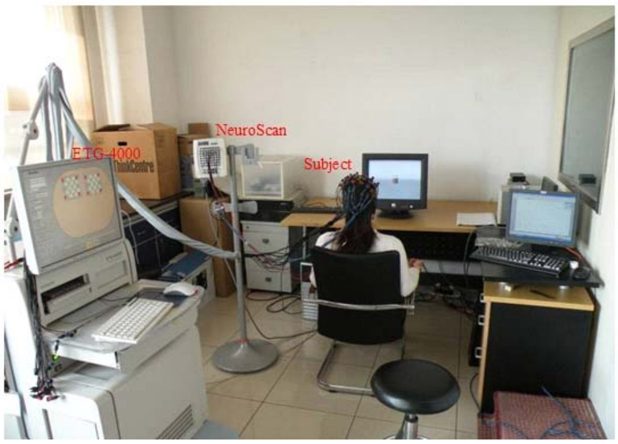

(b)

Fig. 3. The synchronous method and experimental setup for simultaneous acquisition of brain signals by NIRS combined with EEG. (a) Synchronous method for simultaneous acquisition of EEG and cerebral blood oxygenation level signals during imagined force and speed of hand clenching. (b) Experimental setup for simultaneous acquisition of EEG and NIRS from the subject.

This article has been accepted for publication in a future issue of this journal, but has not been fully edited. Content may change prior to final publication. Citation information: DOI 10.1109/TNSRE.2016.2627809, IEEE Transactions on Neural Systems and Rehabilitation Engineering

The experimental setup is shown in Fig. 3(b) (left to right: ETG-4000, Neuroscan SynAmps2, subject, computer presenting the cue, and computer recording EEG). The NIRS signals were sampled at 10 Hz; the EEG signals were sampled at 1000 Hz using a 24 bit A/D converter with a signal frequency band of 0–250 Hz and a notch filter at 50 Hz. EOG (the same band pass and sampling rate as for EEG) was recorded to exclude trials contaminated by eye movements. Electrode impedances were kept below 5 k kΩ.

F. Experimental procedure

The subject sat in a comfortable armchair with his/her arms resting naturally on the armrest 0.7–1 m in front of a computer screen that presented task cues. The experimenter positioned the EEG electrodes and NIRS probes according to the helmet used for collecting brain signals by NIRS combined with EEG, as shown in Fig. 2(d). The subject was first instructed to train himself/herself with a set of trials and then execute 10 runs of formal trials during each session. A start tag "ST" was sent to the ETG-4000 using a serial port, as shown in Fig. 2(a). Each run comprised 6 trials corresponding to 6 different imagined force and speed of hand clenching tasks. Thus, each session had a total of 60 trials and 10 trials for each condition.

The baseline of the first trial in the formal experiment was the resting state from t = 0 s to 20 s, during which cerebral blood oxygenation returned to the baseline state, as shown in Fig. 1. After baseline, a black fixation cross as a preparation prompt appeared on the white screen and lasted for 2 s, during which subjects were asked to stay relaxed and ready for the trial. At t = 22 s, a cue in the form of a picture appeared on the white screen indicating force of hand clenching imagination of 20%/50%/80% MVFG or speed of hand clenching imagination of 0.5 Hz/1 Hz/2 Hz. The cue lasted 2 s, and the subjects were asked to get ready for motor imagery. At the moment when task cues were presented, the synchronized trigger signal was simultaneously sent to the EEG and NIRS amplifier by parallel and serial ports, respectively.

The subject began to execute the cued imagery task when the cued picture disappeared from the screen and a black star-shaped fixed cursor appeared on the white screen. The subject was asked to perform the cued motor imagery task attentively, and they recalled the process of his/her right hand clenching force and maintaining the target force or speed of hand clenching without actual motion. The imagined task was maintained for 10 s until the fixation cursor disappeared from the screen, during which no online identification results were provided for the subject. When the task ended, the screen went blank, and the subject was given an 18–20 s rest until the next trial started. At the end of the experiment, an end tag was sent to the ETG-4000 using the serial port.

A trial lasted 32–34 s including the buffer time. During the trial, subjects were asked to avoid blinking, slow eye movement, and using facial muscles as well as other body parts except during the random rest intervals between trials. Each subject attended 3 sessions and 30 trials for each motor imagery task in the experiment. The trials (different motor imagery tasks) in the study were presented in a randomized sequence using E-Prime.

G. Data processing for NIRS and EEG

1) Data processing for NIRS: We used a continuous wave NIRS, and changes in optical intensity were related to changes in hemoglobin concentrations according to the modified Beer-Lambert law [33]. Changes in concentrations of oxygenated hemoglobin (ΔOxy-Hb) and deoxygenated hemoglobin (ΔDeoxy-Hb) by the dual wavelength system can be estimated using equations (1) and (2), respectively [33].

$$\Delta\text{Oxy-Hb} = \frac{\text{EC}_{\lambda1}^{\text{Hb}}\Delta\text{OD}_{\lambda2} - \text{EC}_{\lambda1}^{\text{Hb}}\Delta\text{OD}_{\lambda1}}{d(\text{EC}_{\lambda1}^{\text{Hb}}\text{EC}_{\lambda2}^{\text{HbO}} - \text{EC}_{\lambda1}^{\text{HbO}}\text{EC}_{\lambda2}^{\text{Hb}})} \quad (1)$$

$$\Delta\text{Deoxy-Hb} = \frac{\text{EC}_{\lambda2}^{\text{HbO}}\Delta\text{OD}_{\lambda1} - \text{EC}_{\lambda2}^{\text{Hb}}\Delta\text{OD}_{\lambda2}}{d(\text{EC}_{\lambda1}^{\text{Hb}}\text{EC}_{\lambda2}^{\text{HbO}} - \text{EC}_{\lambda1}^{\text{HbO}}\text{EC}_{\lambda2}^{\text{Hb}})} \quad (2)$$

$\Delta\text{OD}_{\lambda1}$ and $\Delta\text{OD}_{\lambda2}$ are changes in optical density of wavelengths λ1 and λ2, respectively. $\text{EC}_{\lambda1}^{\text{HbO}}$, $\text{EC}_{\lambda2}^{\text{HbO}}$, and $\text{EC}_{\lambda2}^{\text{Hb}}$ and $\text{EC}_{\lambda1}^{\text{Hb}}$ are the extinction coefficients of oxygenated hemoglobin and deoxygenated hemoglobin for wavelengths λ1 and λ2, respectively, and *d* is the total corrected photon path-length [34]-[36]. In this study, λ1 = 695 nm, λ2 = 830 nm, $\text{EC}_{\lambda1}^{\text{HbO}} = 0.3120$, $\text{EC}_{\lambda1}^{\text{Hb}} = 1.9665$, $\text{EC}_{\lambda2}^{\text{HbO}} = 1.0507$, and $\text{EC}_{\lambda2}^{\text{Hb}} = 0.7804$ were obtained from previous research [33]-[35].

The original optical intensity data were converted into oxyhemoglobin concentration data (HbO/Hb) by NIRS-SPM, which were then low-pass filtered at 0.1 Hz and linearly detrended. The mental tasks performed by subjects were divided into 2 categories including imagined force and speed of hand clenching. The imagined force of hand clenching included 3 classes: 20/50/80% MVGF, and their event identifiers were F1, F2, and F3; the imagined speed of hand clenching had 3 classes including 0.5/1/2 Hz, and their event identifiers were F4, F5, and F6. The different epochs were extracted according to the event identifiers, and the data segments were calibrated with (-12, 0) s as the baseline, and then averaged. NIRS channels 21 and 7 corresponded to EEG channels C3 and C4, respectively. Channels 21 and 7 were investigated because of motor imagery involving the right hand [10].

2) Data processing for EEG: Data preprocessing for EEG included the following: the NeuroScan CNT file was loaded into EEGLAB; the 21 channel electrode location file (21channlocs.ced) was loaded into EEG; only channels C3 and C4 were calculated and extracted in data processing; EEG signals were down-sampled to 250 Hz and notched at 50 Hz; to remove baseline drift and extract more features for further study, an FFT linear filter (0.05-45 Hz) was implemented using EEGLAB's eegfiltfft function to band/low-pass filter EEG; t = 0 s corresponds to the onset of imagined movement parameters task (corresponding to t = 24 s of the first trial in Fig. 1).

After the above data preprocessing, the interesting epochs of 8 s in length from -4 to 4 s were extracted. Event marks 1, 2, and 3 marked 20/50/80% MVGF imagined force of hand clenching movement, respectively; event marks 4, 5, and 6 corresponded to 0.5 Hz, 1 Hz, and 2 Hz speed of hand clenching motor imagery tasks, respectively. The interval might cover the resting state of (-4,-2) s, the movement preparation state of (-2,0) s, and imagined hand clenching movement of (0,4) s.

Then, further processing for the above results included the following: the baseline correction interval was (-2.5, -2) s and was chosen from the resting state interval of (-4, -2) s; EOG and EMG were removed from the epochs with ICA using EEGLAB's binica function; the data were low-pass filtered using eegfiltfft at 2 Hz to extract slow potentials; for each subject, movement-related cortical potentials (MRCP) related to each imagined force and speed of hand clenching movement were calculated by the superimposed and averaged techniques.

H. Features extraction, fusion, statistical analysis, and classification of NIRS-EEG related to imagined force and speed of hand clenching

To take into account the portability and practicality of the hybrid NIRS-EEG BCI system in the future, and also the dimension of the feature vector, NIRS and EEG features were extracted from the C3 and C4 positions, which are representative of the right and left sensorimotor areas.

1) Features extraction for NIRS: Yin et al. demonstrated that the concentration signal was more effective in reflecting brain activations than optical signals [10]. In addition, their research also showed that the difference between HbO and Hb concentrations (HbD) may provide new information for cerebral activations and can achieve better results than the Hb, HbO, and HbT features. Therefore, the HbD and HbO features of 24 channels from the (0, 10) s period were extracted.

2) Features extraction for EEG: Yin et al. showed that the phase feature outperformed the amplitude feature, and the classification accuracy can be improved by the amplitude combined with phase features [10]. To identify different levels of hand clenching force and speed motor imageries, the instantaneous amplitude (IA), instantaneous phase (IP), and instantaneous frequency (IF) of EEG signals were calculated and combined into a feature vector that was expected to enhance classification performance. These features can be extracted using the Hilbert transform [10], [37]. The following (3) shows that a non-stationary signal $x(t)$ is transformed into $y(t)$ by Hilbert transform.

$$y(t) = \frac{1}{\pi} P \int_{-\infty}^{+\infty} \frac{x(\tau)}{t-\tau} d\tau \tag{3}$$

Here, P is Cauchy principal value. IP, IA, and IF can be calculated by the following (4)-(6), respectively

$$\mathrm{IP} = \varphi(t) = \arctan \frac{y(t)}{x(t)} \tag{4}$$

$$\mathrm{IA} = \sqrt{x(t)^2 + y(t)^2} \tag{5}$$

$$\mathrm{IF} = \frac{d\varphi(t)}{dt} \tag{6}$$

3) Features fusion for NIRS-EEG: Classification of a sole feature was widely used in BCI applications. Classification of multi-features fusion was adopted in the current study. Yin et al. showed that the merged feature outperformed the sole EEG feature and the sole fNIRS feature [10]. To identify different levels of hand clenching force and speed motor imageries, NIRS features related to motor parameters imagery, the HbO and HbD, first were combined to construct the HbO-HbD feature, and then EEG features related to motor parameters imagery, the IA, IP, and IF, were integrated to form the IA-IP-IF feature. Finally, the HbO-HbD and the IA-IP-IF were fused to create the HbO-HbD & the IA-IP-IF. A total of 10 features were obtained from fNIRS and EEG (4 features from NIRS and 6 features from EEG).

4) Statistical analysis of NIRS and EEG related to imagined force and speed of hand clenching: We assumed that the main factor influencing NIRS and EEG was imagined force and speed of hand clenching. The influence factor involved 6 levels including 20/50/80% MVGF and 0.5/1/2 Hz imagined hand clenching force and speed. Analysis of variance (ANOVA) of single factor and subsequent multiple comparisons were used on NIRS features (HbO and HbD) and EEG features (IA, IP, and IF). The results of ANOVA and multiple comparisons were considered significant at $P < 0.05$.

5) Classification of imagined force and speed of hand clenching by SVM: Six-class classifications were performed in the study (3 levels of hand clenching force and 3 levels of hand clenching force motor imageries). The support vector machine (SVM) has been widely used in BCI research and applications. In this study, SVM function from MATLAB (version 7.6) was modified according to the literature [38], [39] and used to classify these imagined motor parameters. The core of SVM is to construct the optimal hyper plane so that the classification error of the unknown sample is minimized.

To change the nonlinear inseparable problem into the linear separable problem, the appropriate kernel function was chosen for the classification hyper plane to perform the nonlinear transform. The radial basis kernel function was chosen as the kernel function of SVM.

The SVM function internally determines the hyperparameter for regularization. The fitcecoc function was used to train a multiclass error-correcting output codes model composed of binary SVM learners. The crossval function was used to cross-validate SVM classifiers. To determine the complexity hyperparameter for regularization, 4-folds cross-validation was used to train the SVM. In our experiment, each subject performed 6 types of motor imagery tasks, each of which had 30 trials, for a total of 180 trials. The 180 trials were randomly divided into 4 subsets, each of which had the same number of samples. The samples from 3 randomly selected subsets were used for training, while samples from the remaining subset were used for testing [40]. Therefore, although we conducted a limited number of trials, the randomly selected subset samples can be used repeatedly to train and validate the SVM model. Furthermore, this determines its parameters C and σ through cross-validation. The mean value of the 4 classification results by cross-validation were used as an estimate of classification accuracy.

III. Results

A. Imagined hand clenching force modulating NIRS and EEG

Fig. 4(a) shows the time evolution curve of the averaged HbO and Hb concentrations related to 20/50/80% MVGF imagined tasks at NIRS channel 21 corresponding to the left motor cortex for representative subject S1 (Although there were variations among the 6 subjects, their results showed similar trends.). Fig. 4(a) shows HbO related to 50% and 20% MVGF imagined tasks, indicating a trend toward positive

This article has been accepted for publication in a future issue of this journal, but has not been fully edited. Content may change prior to final publication. Citation information: DOI 10.1109/TNSRE.2016.2627809, IEEE Transactions on Neural Systems and Rehabilitation Engineering

change in the interval (-2, 0) s of preparation for the imagined force of hand clenching task, except for HbO leveling out for 80% MVGF imagination; HbO related to the 3 tasks showed a trend toward negative values with a negative peak in the interval (0, 10) s of execution for the imagined force of hand clenching task and then became positive. After the negative peak, HbO related to 80/50/20% MVGF imagined tasks showed a trend toward positive changes. It had a positive peak approximately 6–8 s after the imagined force of hand clenching tasks ended at t = 10 s. In addition, the variation trend in Hb was approximately opposite that of HbO.

Fig. 4(b) shows the time evolution curve of the averaged EEG related to the 3 imagined force of hand clenching tasks at channel C3 for representative subject S1. Table I shows the variation trend of the potentials related to the 3 conditions in the typical intervals. The variation trends of potentials related to the 3 conditions in different intervals were not identical.

The readiness potentials (RP), which slowly increased toward negative potentials at least 500 ms before movement onset, may represent the planning of a given movement. The motor potentials (MP), which approached negative potentials with steep slope about 150 ms prior to movement onset, may be related to the execution of a given movement. The movement-monitoring potentials (MMP), which varied from negative potentials to positive potentials after movement onset, may be associated with the precision of a given movement [41]. The "(-2000, -1196) NC" denotes that the potentials adopted negative deflection in the -2000 to -1196 ms interval; the "(-70, 596) PC" denotes that the potentials adopted positive deflection in the 70 to 596 ms interval.

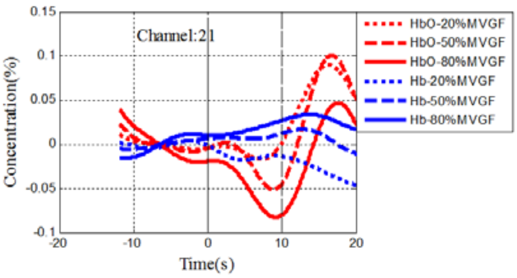

(a)

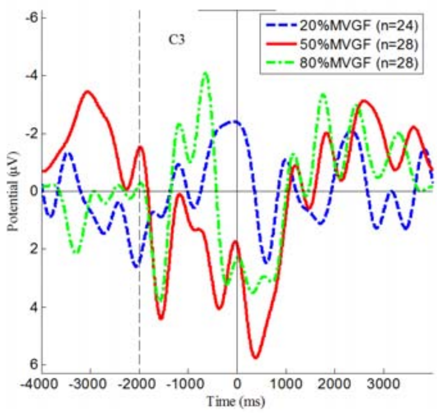

(b)

Fig. 4. Three imagined force of hand clenching parameters (20%/50%/80% MVGF) modulated NIRS and EEG. (a) HbO/Hb at NIRS channel 21. (b) EEG/MRCP at channel C3. The onset of the imagined force of hand clenching tasks was set as t= 0 ms.

B. *Imagined hand clenching speed modulating NIRS and EEG*

Fig. 5(a) demonstrates the time evolution curve of the averaged HbO and Hb concentrations related to 0.5 Hz/1 Hz/2 Hz imagined speed of hand clenching tasks at NIRS channel 21 for representative subject S1. Fig. 5(a) shows HbO related to 1 Hz and 2 Hz imagined speed tasks displaying a trend toward

TABLE I The intervals (ms) and variation trends of readiness potentials (RP), motor potentials (MP), and movement-monitoring potentials (MMP) related to 3 imagined force of hand clenching tasks at channel C3 for representative subject S1. Negative change (NC); Positive change (PC).

	20% MVGF	50% MVGF	80% MVGF
RP	(-2000, -1196) NC	(-1557, -1175) NC	(-1584, -650) NC
MP	(-880, -70) NC	(-364, -44) NC	(-212, 16) NC
MMP	(-70, 596) PC	(-44, 376) PC	(16, 312) PC

negative change in the interval (-2, 0) s of preparation for the imagined speed of hand clenching tasks and a negative peak in the interval (0, 10) s of execution for the imagined speed of hand clenching tasks. After the negative peak, HbO related to 1 Hz and 2 Hz imagined tasks had a positive change and reached a positive peak at approximately 6–8 s after the imagined speed of hand clenching tasks ended at t = 10 s.

Imagined hand clenching at the slow speed of 0.5 Hz seemed to be special. The related HbO had a negative peak in the interval (-5, 0) s and then began slow positive changes, reaching a positive peak about 8 s after imagined movement ended at 10 s.

Fig. 5(b) reveals the time evolution curve of the averaged EEG related to the 3 imagined speed of hand clenching tasks at channel C3 for representative subject S1. Table II shows the variation trend of the potentials related to the 3 conditions in the typical intervals.

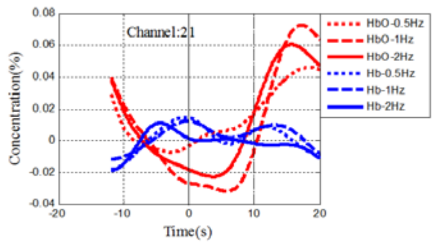

(a)

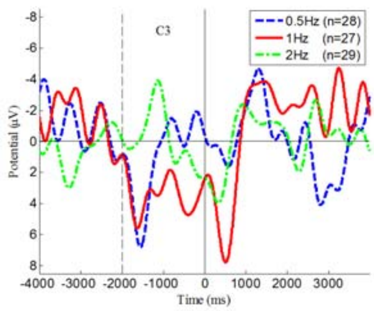

(b)

Fig. 5. Three imagined speed of hand clenching parameters (0.5/1/2 Hz) modulated NIRS and EEG. (a) HbO/Hb at NIRS channel 21. (b) EEG/MRCP at channel C3. (c) HbO/Hb at NIRS channel 7. (d) EEG/MRCP at channel C4. The onset of the imagined speed of hand clenching tasks was set as t = 0 ms.

This article has been accepted for publication in a future issue of this journal, but has not been fully edited. Content may change prior to final publication. Citation information: DOI 10.1109/TNSRE.2016.2627809, IEEE Transactions on Neural Systems and Rehabilitation Engineering

C. Statistical analysis of NIRS and EEG related to imagined force and speed of hand clenching

Below the significance level of 0.05, the value of the statistic F is greater than the critical value $F_{0.05}(5, 24) = 2.62$, so the probability $P < 0.05$. This indicated that the tested factor of imagined hand clenching force and speed had a significant impact on NIRS (HbO and HbD) and EEG (IA, IP, and IF).

TABLE II The intervals (ms) and variation trends of readiness potentials (RP), motor potentials (MP), and movement-monitoring potentials (MMP) related to 3 imagined speed of hand clenching tasks at channel C3 for representative subject S1. Negative change (NC); Positive change (PC).

	0.5 Hz	1 Hz	2 Hz
RP	(−1556, −796) NC	(−1632, −830) NC	(−1820, −1136) NC
MP	(−500, −196) NC	(404, 76) NC	(1136, 330) NC
MMP	(−196, 572) PC	(76, 504) PC	(330, 925) PC

D. Classification for imagined force and speed of hand clenching by NIRS, EEG, and NIRS-EEG

Based on the materials and methods proposed in this paper, after investigating imagined force and speed of hand clenching modulation of brain activity using NIRS combined with EEG, multi-levels of imagined movement parameters (a total of 6 classes) were classified by the fusion features of NIRS and EEG using SVM to explore potential application in the field of BCI.

The identification accuracies for 3 levels of hand clenching force and 3 levels of hand clenching speed motor imageries (6 class-classifications) based on NIRS (HbO-HbD), EEG (IA-IP-IF), and NIRS-EEG (HbO-HbD & IA-IP-IF) merged features by SVM are shown in Table III and Fig. 6. The average classification accuracies across 6 subjects by the HbO-HbD feature combination of NIRS, the IA-IP-IF feature combination of EEG, and the HbO-HbD & IA-IP-IF of NIRS-EEG feature combination were 0.64 ± 0.04, 0.72 ± 0.03, and 0.74 ± 0.02, respectively. Compared with accuracies of non-trained, those of trained by the HbO-HbD, the IA-IP-IF, and the HbO-HbD & IA-IP-IF were 0.69 ± 0.01, 0.74 ± 0.01, and 0.75 ± 0.01, respectively.

TABLE III. Identification accuracies for 3 levels of hand clenching force and 3 levels of hand clenching speed motor imageries (6 class-classifications) based on NIRS (HbO-HbD), EEG (IA-IP-IF), and NIRS-EEG (HbO-HbD & IA-IP-IF) features by SVM.

Subject	S1	S2	S3	S4	S5	S6	Trained	Non-trained	All
HbO-HbD	0.66 ± 0.05	0.64 ± 0.03	0.60 ± 0.04	0.62 ± 0.03	0.64 ± 0.03	0.68 ± 0.04	0.69 ± 0.01	0.63 ± 0.02	0.64 ± 0.04
IA-IP-IF	0.73 ± 0.04	0.70 ± 0.02	0.71 ± 0.05	0.72 ± 0.03	0.74 ± 0.04	0.72 ± 0.01	0.74 ± 0.01	0.71 ± 0.01	0.72 ± 0.03
HbO-HbD &IA-IP-IF	0.73 ± 0.02	0.71 ± 0.01	0.72 ± 0.02	0.74 ± 0.03	0.78 ± 0.01	0.77 ± 0.02	0.75 ± 0.01	0.73 ± 0.02	0.74 ± 0.02

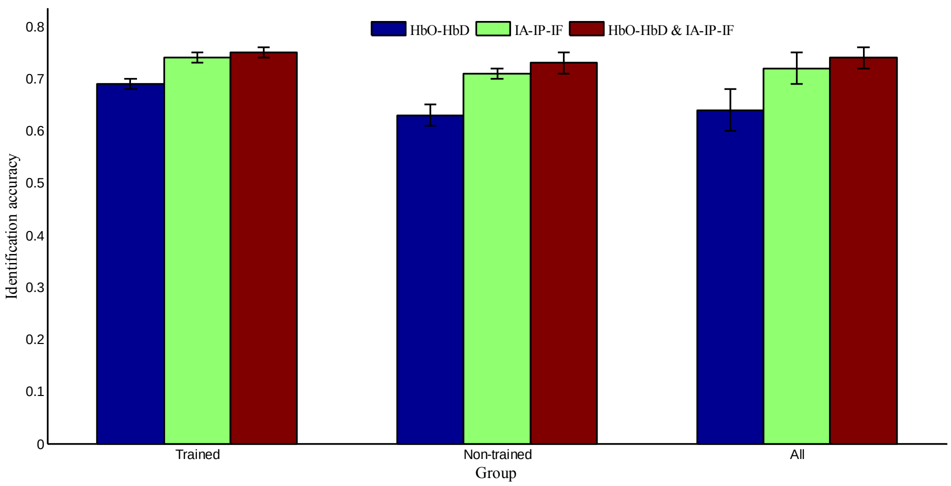

Fig. 6. Identification accuracies for 3 levels of hand clenching force and 3 levels of hand clenching speed motor imageries based on NIRS (HbO-HbD), EEG (IA-IP-IF), and NIRS-EEG (HbO-HbD & IA-IP-IF) features by SVM. Identification accuracy varied with different groups.

IV. Discussion

Differing from the previous single measurement method or combined method without measuring the same brain position [11], this study made full use of the optical probe spacing of 3 cm and detection region located in the intermediate area between the emitter and detector [13]. In addition, the present study took into account the effects of EEG electrode diameter (1 cm) and NIRS probe diameter (2–3 mm) and placed the EEG electrodes in the intermediate area between the NIRS probes (Fig. 2) to measure synchronously EEG activity and the corresponding NIRS activity. Therefore, EEG electrodes and

This article has been accepted for publication in a future issue of this journal, but has not been fully edited. Content may change prior to final publication. Citation information: DOI 10.1109/TNSRE.2016.2627809, IEEE Transactions on Neural Systems and Rehabilitation Engineering

optical probes can share the same measurement location with the proposed method. The single neuroimaging method has advantages, but it is difficult to overcome its inherent limitations [12]. A neuroimaging method that combines the 2 acquisition methods was required to acquire simultaneously activation related to cognitive activities in the same brain area.

NIRS has a significant problem that was confirmed by the study. There was a long delay (6–10 s) in the hemodynamic responses (as shown in Figs. 4 and 5), which lagged behind a specific sensation, perception, and cognitive activity [3]. Therefore, the method of NIRS combined with EEG must solve the problem of long delay in the hemodynamic response. This problem may be alleviated by appropriate data fusion methods. The information transmission rate of BCI based on NIRS combined with EEG may suffer from the poor response time of NIRS [11]. However, the classification accuracy for mental activities based on NIRS combined with EEG may be improved by their complementary information content [11]. NIRS indirectly characterizes neural activity by the hemodynamic response to brain activity; conversely, EEG directly reflects neural activity. However, their mechanisms are different and they involve 2 different types of signals. The differences between them usually result in different classification results for motor imagery. The proposed method of simultaneously measuring activity in the same area of the brain using NIRS combined with EEG may provide further support for mutual complementation of the 2 types of data.

In addition, as shown in Figs. 4 and 5, compared with EEG, the HbO signal is relatively stable, subject to little contamination such as eye movement (evoking EOG) and body movement (evoking EMG), and has a relatively high signal to noise ratio. There are some significant differences in the amplitude and peak of HbO related to 3 imagined force and speed of hand clenching tasks. However, compared with NIRS signals, EEG displays intense oscillations, strong non-stationarity, large variability, and predominantly spontaneous activity, which may drown the small modal in EEG. In addition, EEG has a low signal to noise ratio and is susceptible to strong artifact contamination such as EOG, EMG, line noise, and micro-movement of cables. Although EEG and NIRS have low spatial resolution (1–2 cm) [11], NIRS may discriminate activations from different brain areas more accurately than EEG. Finally, EEG has good time resolution and thus a short delay in response to 3 imagined force and speed of hand clenching movements and may, to a certain extent, almost characterize in real time the latency of the positive and negative peaks related to 3 imagined force and speed of hand clenching (as shown in Tables I and II).

Fig. 4(a) shows that imagined hand clenching force modulated NIRS signals. HbO concentrations in response to different imagined force of hand clenching tasks had different negative peaks, positive peaks, and latencies. In the interval (0, 10) of 3 imagined hand clenching force tasks, HbO displayed a negative change and had a negative peak at the left motor cortex (NIRS channel 21). The order for the negative peak (NP) magnitude from high to low was NP_{20}, NP_{50}, and NP_{80}, and the order for the negative peak latency (NPL) from long to short was NPL_{80}, NPL_{50}, and NPL_{20}. After the negative peak, HbO responses to 3 imagined hand clenching force tasks trended to positive changes and a positive peak about 6–8 s after motor imagery ended (t = 10 s). The order for the positive peak (PP) magnitude from high to low was PP_{50}, PP_{20}, and PP_{80}; the order for the positive peak latency (PPL) from long to short was PPL_{80}, PPL_{50}, and PPL_{20}. EEG at C3 did bring a corresponding change in HbO at NIRS channel 21 (EEG at C3 did not correspond to HbO at NIRS channel 21). This may be because there are 2 types of signal. EEG can directly reflect electrical activity of neurons in the brain, while NIRS may indirectly reflect brain activity by detecting variation in HbO/HbR concentration based on the neurovascular coupling hypothesis. Therefore, they are not directly comparable, but their information content can be complementary. In the interval (-2000, 1000) ms, EEG related to 3 imagined hand clenching forces may reflect neural processing of movement readiness, execution, and monitoring, which occurred in different intervals. This may embody the advantage of EEG time resolution, but EEG spontaneously oscillated and suffered from contamination. Three imagined hand clenching force tasks modulating brain signals in the right motor cortex (NIRS channel 7 and EEG electrode C4) were similar to Fig. 4 (a) and (b).

Fig 5(a) shows that imagined speed of hand clenching modulated NIRS signals. HbO concentrations in response to different imagined speed of hand clenching tasks had different negative peaks, positive peaks, and latencies. In the interval (0, 10) of imagined speed of hand clenching tasks, HbO related to imagined hand clenching at 1 Hz and 2 Hz exhibited a negative change and a negative peak in the left motor cortex (NIRS channel 21). The order for the negative peak (NP) magnitude from high to low was NP_{2Hz} and NP_{1Hz}; the order for the negative peak latency (NPL) from long to short was NPL_{1Hz} and NPL_{2Hz}. After the negative peak, HbO in response to imagined speed of hand clenching tasks trended to positive changes and had a positive peak about 6–8 s after motor imagery ended (t = 10 s). The order for the positive peak (PP) magnitude from high to low was PP_{1Hz} and PP_{2Hz}, while the order for the positive peak latency (PPL) from long to short was PPL_{1Hz}, and PPL_{2Hz}. Three imagined speed of hand clenching tasks modulating brain signals in the right motor cortex (NIRS channel 7 and EEG electrode C4) were similar to Fig. 5(a) and (b). HbO related to imagined hand clenching at 0.5 Hz mainly displayed a rising trend towards the positive, a typical HbO behavior, for which there is no appropriate interpretation at this time. Normally, the typical behavior of variation in hemoglobin concentration was such that HbO increased while HbR decreased in an approximate mirror fashion during brain activation [11]. In addition, the increase in HbO related to brain activation lagged behind brain activation with a long time delay of about 6–10 s. The results of this study showed a distinct pattern of hemoglobin response in which HbO initially exhibited a decline and then a rise during imagined force and speed of hand clenching tasks (as shown in Figs. 4 and 5). The initial decline in HbO concentration may be due to oxygen consumption by neuronal activation, but consumption of oxygen causes an increase in blood supply, which in turn leads to a rise in HbO concentration. These phenomena may be caused by the effect of blood over-perfusion. HbO had a positive peak at about 6–8 s after imagined force and speed of hand clenching movement ended, which is consistent with results based on fNIRS and fMRI [11]. The lagging positive changes in HbO also reflect mental activities for imagined force and speed of hand clenching movement or imagined hand clenching force and speed modulating HbO. In addition, in contrast to HbO, HbR showed a slow rising trend and a decline during imagined force and speed of hand clenching movement.

The analysis showed that the activity pattern over all of the subjects in these channels had certain variability because of differences between the subjects. Although channels 7 and 21 and C3 and C4 were not the only active channels for NIRS and EEG, their representations of motor areas were mainly analyzed in the current study and as few channels as possible were considered for decoding imagined hand clenching force and speed.

For identification of right hand clenching force and speed parameters imagery, Table III shows that the IA-IP-IF combination feature outperformed the HbO-HbD combination feature by 8% for the average of all subjects. This may indicate that EEG, which directly reflects electrical activity of neurons, differs from NIRS, which detects a metabolic signal that indirectly reflects neuronal activity. The 2 techniques have different information content. Table III also shows that the HbO-HbD & IA-IP-IF combination feature outperformed the HbO-HbD and the IA-IP-IF combination feature by 10% and 2% for the average of all subjects, respectively. This result may also indicate that EEG is complementary to NIRS and that combining the 2 methods can improve classification accuracy.

Additionally, Table III shows that the classification accuracies of the 6 subjects were not the same. The main reason for this is in the differences of each subject's mental activity for imagined hand clenching at a specific speed or force. This resulted in EEG and NIRS differences, which yielded differences in classification features and results. Table III also shows that the classification accuracies of trained subjects were better than those of subjects without training (2 to 6% improvement). Furthermore, using a combination of NIRS and EEG improved classification accuracy compared to using the single mode NIRS or EEG (1 to 10% improvement).

Moreover, as shown in Table III, classification accuracy of the trained group outperformed that of the non-trained one by 2–6%. This may demonstrate that training subjects increases separation of features, and good training is expected to further improve classification accuracy.

In short, the NIRS-EEG fusion feature (HbO-HbD & IA-IP-IF) improves accuracy of decoding imagined movement parameters, and it is expected to provide more instructions for BCIs to naturally control devices such as manipulators. However, further improvement in classification accuracy of imagined movement parameters is required. The measures to be taken are: (1) improving the NIRS-EEG signal to noise ratio by designing an adaptive preprocessing algorithm, and 2) online training of subjects and producing a significant difference between NIRS-EEG features evoked by motor parameters imagery.

Compared with studies of combined NIRS-EEG decoding of motor imagery or movement directions [10], [29-31], the present study attempted to identify imagined force and speed (such as imagined hand clenching force and speed) by simultaneously collecting NIRS and EEG data from the same motor area. The averaged and maximum accuracy for decoding imagined hand clenching force and speed (6 classes) using the fusion features of HbO-HbD & IA-IP-IF were 0.74 ± 0.02 and 0.78 ± 0.01, respectively. It is expected that this study may improve classification accuracy of imagined grip strength and speed and provide increased control commands of force and speed for brain-controlled robots.

Although the fusion of multi-mode signals may outperform sole NIRS or sole EEG, the fusion method choice is important for improving the hybrid BCI based on NIRS-EEG. It is noteworthy that several recent methods tackle multivariate signal analysis on other levels instead of a feature fusion level [42]-[45]. In our future work, these new methods will be applied to merge NIRS and EEG signals to increase the accuracy of the hybrid BCI.

In addition to the above discussion, many channels are related to motor imagery tasks, and the combination of multi-channels information may increase classification accuracy [46]. However, the use of fewer-channels analysis is out of consideration for future studies due to the portability and comfort issues accompanying the hybrid NIRS-EEG BCI helmet. Although this method attempts to achieve the hybrid NIRS-EEG BCI with few NIRS probes and EEG electrodes, subjects would feel uncomfortable wearing the multi-channel hybrid NIRS-EEG BCI helmet, and would feel pain after wearing it for an extended time. This discomfort and pain is due to spring pressure applied to NIRS probes on the scalp.

In addition to the above problems, other questions to be discussed, which are how to control motor imagery experiments and how to determine whether subjects performed the required imagery task according to instructions, have remained a bottleneck in BCI based on motor imagery research. These questions are also the key to BCI research and its practical application. Furthermore, this involves how to quantitatively measure the effect or result of motor imagery mental activity. A common problem faced by all experiments of BCI based on motor imagery (including simple motor imagery involving the right and left hands) is the controllability, observability, and stability or reliability of the motor imagery BCI experiment. Motor imagery is an endogenous, active (or subjective) mental activity performed by subjects without overt actual movement. Therefore, the experimenter cannot determine whether the subjects imagined the movement or how well they performed a specific imagination. Neurofeedback presented to the subjects is the result of BCI algorithms, and thus the decoding methods may present inaccurate results. Furthermore, for the development of BCI systems based on motor imagery, BCI illiteracy is of great challenge. Therefore, the methods or systems of highly efficient training subjects or users is a key technology for this kind of BCI system. Thus, the design of the experimental paradigm should be improved in our future work.

In detail, due to differences in imagination ability, motor imagery between different subjects shows considerable difference. Even if subjects performed the same imagery task, the resulting NIRS and EEG signals were different. Therefore, the feasibility of the superposition of trials was considered, and the analysis and interpretation of results required caution. Additionally, there was also a difference in the execution of the same cued motor imagery mental task at different times by a specific subject. To this end, the BCI illiteracy related to motor imagery is a great challenge [47]-[50]. This may require customizing a specific BCI system for the specific subject and providing specific training. Finally, the PC, NC, and other components in Table II show a representative subject (S1). Although, there are variations in the timeline for different subjects, they demonstrate some similar trends in signal changes.

In the current study, only 6 subjects participated in the experiment. After positioning EEG electrodes and NIRS probes, it took longer to reduce EEG electrode impedance and adjust the intensity of the emission and detection NIRS probes compared with a single mode acquisition method, which may have affected a subject's state. Therefore, further exploration with a larger group of subjects is necessary to increase confidence in the findings. The present results were analyzed offline, and further research will use online analysis.

V. Conclusion

A method for simultaneously measuring activation in the same brain area using NIRS combined with EEG during specific cognitive activities was presented and proven feasible and effective. The acquisition method takes advantage of the HbO signal, which is relatively stable with little movement interference, a relatively high signal to noise ratio, and relatively accurate spatial positioning, as well as EEG's timely response to mental activities. It may provide a means for integrating NIRS and EEG information content.

The experimental study showed that imagined hand clenching force and speed modulated NIRS signals using the proposed acquisition method. There were different negative peaks, positive peaks, and latencies of HbO concentrations in response to different imagined force and speed of hand clenching movement tasks. In the interval (0, 10) s for executing imagined force and speed of hand clenching movement tasks, HbO initially exhibited a negative deflection and a negative peak followed by a positive deflection and a positive peak at about 6–8 s when motor imagery ended at t = 10 s. EEG related to different imagined force and speed of hand clenching in the interval (-2, 1) s may reflect brain neural processing of readiness, execution, and monitoring of a given hand clenching movement imagination. Although these modalities seemed to have no influence on each other, NIRS combined with EEG measuring the same brain area may yield useful information on electrical activity as well as local hemodynamics.

NIRS and EEG reflect activity of neurons from different perspectives. Comparison of classification results between combined features may indicate that NIRS and EEG complement each other, and NIRS-EEG can improve classification accuracy of multi-levels of imagined movement parameters. Furthermore, the results show that improvement of classification accuracy of imagined movement parameters depends on the effective training of subjects.

Our future studies include: 1) Integrating and miniaturizing the acquisition method of NIRS combined with EEG to achieve a portable NIRS-EEG acquisition system, 2) Developing an online BCI system based on NIRS-EEG induced by motor parameters imagery and improving performance of the system by training subjects using neural feedback.

Acknowledgments

The authors would like to thank Lili Pei and Yanhua Yang for participating in experiment sessions.

References

[1] F. Scholkmann, S. Kleiser, A. J. Metz, R. Zimmermann, J. Mata Pavia, U. Wolf, and M. Wolf, "A review on continuous wave functional near-infrared spectroscopy and imaging instrumentation and methodology," *NeuroImage*, vol. 85, Pt 1, pp. 6-27, Jan. 2014.

[2] M. Izzetoglu, K. Izzetoglu, S. Bunce, H. Ayaz, A. Devaraj, B. Onaral, and K. Pourrezaei, "Functional near-infrared neuroimaging," *IEEE Trans. Neural. Syst. Rehab. Eng.*, vol. 13, no. 2, pp. 153–159, Jun. 2005.

[3] Y. Hoshi, "Functional near-infrared spectroscopy: current status and future prospects," *J. Biomed. Opt.*, vol. 12, no. 6, 062106, Nov-Dec. 2007.

[4] X. Cui, S. Bray, D. M. Bryant, G. H. Glover, and A. L. Reiss, "A quantitative comparison of NIRS and fMRI across multiple cognitive tasks," *NeuroImage*, vol. 54, no.4, pp. 2808–2821, Feb. 2011.

[5] S. M. Coyle, T. E. Ward, C. M. Markham, and G. McDarby, "On the suitability of near-infrared (NIR) systems for next-generation brain-computer interfaces," *Physiol. Meas.*, vol. 25, no. 4, pp. 815-822, Aug. 2004.

[6] S. M. Coyle, T.E. Ward, and C. M. Markham, "Brain–computer interface using a simplified functional near-infrared spectroscopy system," *J. Neural. Eng.*, Vol. 4, no. 3, pp. 219–226 Sep. 2007.

[7] R. Sitaram, H. Zhang, C. Guan, M. Thulasidas, Y. Hoshi, A. Ishikawa, K. Shimizu, and N. Birbaumer, "Temporal classification of multichannel near-infrared spectroscopy signals of motor imagery for developing a brain-computer interface," *NeuroImage*, vol. 34, no. 4, pp. 1416-1427, Feb. 2007.

[8] N. Naseer, and K. S. Hong, "Classification of functional near-infrared spectroscopy signals corresponding to the right- and left-wrist motor imagery for development of a brain–computer interface," *Neurosci. Lett.*, vol. 553, pp. 84– 89, Oct. 2013.

[9] R. Sitaram, S. LEE, and N. Birbaumer, "BCIs that use brain metabolic signals," in *Brain–computer interfaces: principles and practice*, 1st ed., J. R. Wolpaw, and E. W. Wolpaw, Ed. New York: Oxford, 2012, pp. 302-308.

[10] X. Yin, B. Xu, C. Jiang, Y. Fu, Z. Wang, H. Li, G. Shi, "A hybrid BCI based on EEG and fNIRS signals improves the performance of decoding motor imagery of both force and speed of hand clenching," *J Neural Eng.*, vol. 12, no. 3, 036004, Jun. 2015.

[11] S. Fazli, J. Mehnert, J. Steinbrink, G. Curio, A. Villringer, K. R. Müller, and B. Blankertz, "Enhanced performance by a hybrid NIRS–EEG brain computer interface," *NeuroImage* , vol. 59, no. 1, pp. 519–529, Jan. 2012.

[12] G. Pfurtscheller, B. Z. Allison, C. Brunner, G. Bauernfeind, T. Solis-Escalante, R. Scherer, T. O. Zander, G. Mueller-Putz, C. Neuper, and N. Birbaumer, "The hybrid BCI," *Front. Neurosci.*, vol. 4, pp. 1-11, Apr. 2010.

[13] D. J. Leamy, and T. E. Ward, "A novel co-locational and concurrent fNIRS/EEG measurement system: design and initial results," in *Proc. IEEE Eng. Med. Biol. Soc.*, 2010, pp. 4230-4233.

[14] R. Cunnington, R. Iansek, J. L. Bradshaw, and J. G. Phillips, "Movement-related potentials associated with movement preparation and motor imagery," *Exp. Brain Res.*, vol. 111, no. 3, pp. 429-436, Oct. 1996.

[15] J. Decety, "The neurophysiological basis of motor imagery," *Behav. Brain Res.*, vol. 77, no. (1-2), pp. 45-52, May 1996.

[16] G. Pfurtscheller, and F. H. Lopes da Silva, "Event-related EEG/MEG synchronization and esynchronization: basic principles," *Clin. Neurophysiol.*, vol. 110, no. 11, pp. 1842-1857, Nov. 1999.

[17] G. Pfurtscheller, and C. Neuper, "Motor imagery and direct brain-computer communication," *P. IEEE*, vol. 89, pp. 1123-1134, 2001.

[18] C. Neuper, M. WÄortz, and G. Pfurtscheller, "ERD/ERS patterns reflecting sensorimotor activation and deactivation," *Prog. Brain Res.*, vol. 159, pp. 211-222, 2006.

[19] O. F. do Nascimento, K. D. Nielsen, and M. Voigt, "Movement related parameters modulate cortical activity during imaginary isometric plantar-exions," *Exp. Brain Res.*, Vol. 171, no. 1, pp. 78-90, May 2006.

[20] S. C. Wr iessnegger, J. Kurzmann, and C. Neuper, "Spatio-temporal differences in brain oxygenation between movement execution and imagery: a multichannel near-infrared spectroscopy study," *Int. J. Psychophysiol.*, vol. 67, no. 1, pp. 54–63, Jan. 2008.

[21] N. K. Iwata, K. Sakai, and Y. Ugawa, "Correlation between force and motor cortical activation measured by near-infrared spectroscopy (NIRS)," *Neuroimage*, vol. 13, pp. 1196-1196, 2001.

[22] I. Nambu, R. Osu, E. Naito, and M. Kawato, "Relationship between finger-pinch force and motor activation: Comparison between NIRS with fMRI," *IEICE Technical Report Neurocomputing*, vol. 104, pp. 25-30, 2005.

[23] I. Nambu, R. Osu, S. Ando, E. Naito, and M. Kawato, "Prediction for finger force from cortical activity measured by near-infrared spectroscopy (NIRS)," *Neurosci. Res.*, 58S, S128, 2007

[24] I. Nambu, R. Osu, S. Ando, M. Sato, E. Naito, and M. Kawato, "Reconstruction of finger force from NIRS signal-Methodological perspective," *Neurosci. Res.*, 61S, S212, 2008.

[25] I. Nambu, R. Osu, M. A. Sato, S. Ando, M. Kawato, and E. Naito, "Single-trial reconstruction of finger-pinch forces from human motor-cortical activation measured by near-infrared spectroscopy (NIRS)," *Neuroimage*, vol. 47, no. 2, pp. 628-637, Aug. 2009.

[26] S. Waldert, L. Tüshaus, C. P. Kaller, A. Aertsen, and C. Mehring, "fNIRS Exhibits Weak Tuning to Hand Movement Direction," *Plos. One.*, vol. 7, no. 11, e49266, 2012

[27] H. Yuan, C. Perdoni, and B. He, "Relationship between speed and EEG activity during imagined and executed hand movements," *J Neural. Eng.*, vol. 7, no. 2, 26001, Apr. 2010.

[28] Y. Gu, K. Dremstrup, D. Farina, "Single-trial discrimination of type and speed of wrist movements from EEG recordings," *Clin. Neurophysiol.*, vol. 120, no. 8, pp. 1596–1600, Aug. 2009.

[29] Y. Tomita, F.-B. Vialatte, G. Dreyfus, Y. Mitsukura, H. Bakardjian, and A. Cichocki, "Bimodal BCI using simultaneously NIRS and EEG," *IEEE Trans. Biomed. Eng.*, vol. 61, no. 4, pp. 1274-1284, Apr. 2014.

[30] Y. Blokland, L. Spyrou, D. Thijssen, T. Eijsvogels, W. Colier, M. Floor-Westerdijk, R. Vlek, J. Bruhn, and J. Farquhar, "Combined EEG-fNIRS decoding of motor attempt and imagery for brain switch control: An offline study in patients with tetrapegia," *IEEE Trans. Neural Syst. Rehabil. Eng.* vol. 22, no. 2, pp. 222-229, Mar. 2014.

[31] M. J. Khan, M. J. Hong, and K.-S. Hong, "Decoding of four movement directions using hybrid NIRS-EEG brain-computer interface," *Front. Hum. Neurosci*., vol. 8, no. 244, pp. 1-10, Apr. 2014.

[32] R. Roberts, N. Callow, L. Hardy, D. Markland, and J. Bringer, "Movement imagery ability: development and assessment of a revised version of the vividness of movement imagery questionnaire," *J. Sport Exerc. Psychol.*, vol. 30, no. 2, 200-221, Apr. 2008.

[33] J. G. Kim, M. N. Xia, H. L. Liu, "Extinction coefficients of hemoglobin for near-infrared spectroscopy of tissue," *IEEE Eng. Med. Biol. Mag.*, vol. 24, no. 2, pp. 118-121, Mar. 2005.

[34] M. Cope, "The development of a near infrared spectroscopy system and its application for non invasive monitoring of cerebral blood and tissue oxygenation in the newborn infant" Ph.D. dissertation, Dept of Med. Phys. and Biol., Univ. Coll. London, London, UK, 1991.

[35] A. Duncan, J. H. Meek, M. Clemence, C. E. Elwell, L. Tyszczuk, M. Cope, and D. T. Delpy, "Optical path length measurements on adult head, calf and forearm and the head of the newborn infant using phase resolved optical spectroscopy," *Phys. Med. Biol.*, vol. 40, pp. 295–304, Feb. 1995.

[36] D. T. Delpy, M. Cope, D. Z. P Van, S. Arridge, S. Wray, and J. Wyatt, "Estimation of optical pathlength through tissue from direct time of flight measurement," *Phys. Med. Biol.*, vol. 33, no. 12, pp. 1433–1442, Dec. 1988.

[37] Q. M. Le Van, J. Foucher, J. Lachaux, E. Rodriguez, A. Lutz, J. Martinerie and F. J. Varela, "Comparison of Hilbert transform and wavelet methods for the analysis of neuronal synchrony," *J. Neurosci. Meth.*, vol. 111, no. 2, pp. 83–98, Oct. 2011.

[38] S.-Y. Yang, Pattern Recognition and Intelligent Computing: Matlab Technology Realization. Beijing, China: Publishing House of Electronics Industry, 2011.

[39] D. Farina, O. F. do Nascimento, M. F. Lucas, and C. Doncarli, "Optimization of wavelets for classification of movement-related cortical potentials generated by variation of force-related parameters," *J. Neurosci. Meth.*, vol. 162, no. 1-2, pp. 357-363, May 2007.

[40] S. Lemm, B. Blankertz, T. Dickhaus, and K. R. Muller, "Introduction to machine learning for brain imaging," *NeuroImage*, vol. 56, no. 3, pp. 387-399, May 2011.

[41] S. M Slobounov, and W. J. Ray, "Movement-related potentials with reference to isometric force output in discrete and repetitive tasks," *Exp Brain Res.*, vol. 123, no. 4, pp. 461–473, Dec. 1998.

[42] S. Daehne, F. BieQmann, W. Samek, S. Haufe, D. Goltz, C. Gundlach, A. Villringer, S. Fazli, and K. R. Muller, "Multivariate machine learning methods for fusing multimodal functional neuroimaging data," *P. IEEE*, vol. 103, no.9, pp.1507-1530, Sep. 2015.

[43] S. Fazli, S. Daehne, W. Samek, F. BieQmann, and K. R. Muller, "Learning from more than one data source: data fusion techniques for sensorimotor rhythm-based brain–computer interfaces," *P. IEEE*， vol. 103, no. 6, pp. 891-906, Jun. 2015.

[44] K. Uludag , and A. Roebroeck, "General overview on the merits of multimodal neuroimaging data fusion,". *NeuroImage*, vol. 102, pp. 3–10, Nov. 2014.

[45] J. Sui, T. Adali, Q. Yu, J. Chen, and V. D. Calhoun, "A review of multivariate methods for multimodal fusion of brain imaging data," *J. Neurosci. meth.*, vol. 204, no. 1, pp. 68– 81, Feb. 2012.

[46] D. Yao, "A method to standardize a reference of scalp EEG recordings to a point at infinity," *Physiol. Meas.* vol. 22, no. 4, pp. 693–711, Nov. 2001.

[47] X. Liao, D. Yao, D. Wu, and C. Li, "Combining Spatial Filters for the Classification of Single-Trial EEG in a Finger Movement Task,". *IEEE Trans. Biomed. Eng.*, vol. 54, no. 5, pp. 821-831, May 2007.

[48] L. Xu, P. Yang, and D. Yao, "An empirical bayesian framework for brain-computer interfaces," *IEEE Trans. Neural. Syst. Rehabil. Eng.*, vol. 17, no. 6, pp. 521-529, Dec. 2009.

[49] R. Zhang, P. Xu, R. Chen, F. Li, L. Guo, P. Li, T. Zhang, and D. Yao, "Predicting Inter-session Performance of SMR-Based Brain–Computer Interface Using the Spectral Entropy of Resting-State EEG,". *Brain Topogr.*, vol. 28, no. 5, pp. 680-690, Sep. 2015.

[50] R. Zhang, D. Yao, P. A. Valdés-Sosa, F. Li, P. Li, T. Zhang, T. Ma, Y. Li, and P. Xu, "Efficient resting-state EEG network facilitates motor imagery performance," *J. Neural Eng.*, vol. 12, no. 6, 066024, Dec. 2015

Yunfa Fu received the M.S. degree in information engineering from Kunming University of Science and Technology (KMUST), in 2003, and the Ph.D. degree in pattern recognition and intelligent system from University of Chinese Academy of Sciences, in 2012.

His research interests include brain-computer interface and restoration of movement.

Xin Xiong received the Ph.D. degree from school of Sino-Dutch Biomedical &Information Engineering, Northeast University, in 2014.

Her research interest covers medical image processing and pattern recognition, brain network connectivity, brain information processing, and brain-computer interaction.

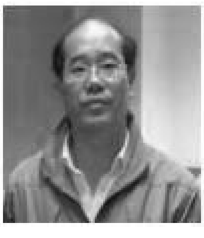

Changhao Jiang received the Ph.D. degree in Psychology from Capital Normal University, in 2006.

His research interest covers the neural mechanisms of sports fatigue and the effect of exercise on mood and executive function by motor brain imaging with event-related potentials and near infrared imaging technology.

Baolei Xu received the Ph.D. degree in pattern recognition and intelligent system from University of Chinese Academy of Sciences, in 2014.

His research interest covers EEG-NIRS based brain-controlled robot interface, biomedical signal processing, and pattern recognition.

This article has been accepted for publication in a future issue of this journal, but has not been fully edited. Content may change prior to final publication. Citation information: DOI 10.1109/TNSRE.2016.2627809, IEEE Transactions on Neural Systems and Rehabilitation Engineering

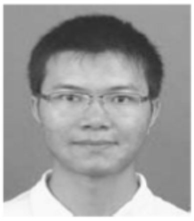

Yonghcheng Li received the Ph.D. degree in pattern recognition and intelligent system from University of Chinese Academy of Sciences, in 2016.

His research interest covers EEG based brain-controlled robot interface, rehabilitation robots, neural interface, neurorobots, and biomedical signal processing.

Hongyi Li received the Ph.D. degree from Harvard University, in 2004.

His research interest covers human-machine integration and medical robot system.